Proceedings of IASS-IWSS 2026 — September 14-18, 2026, Turin, Italy
"R-Evolution of Shapes: Sustainability, Re-Use, and new Design Paradigms"
Annual Symposium of the International Association for Shell and Spatial Structures
3rd Italian Workshop on Shell and Spatial Structures
A. Manuello Bertetto, S. Gabriele, F. Marmo, A. Micheletti (eds.)

Bending-active gabions: a computational form-finding framework for structural upcycling of concrete rubble

Kwong Lau HUNG, Shuaizhong WANG*

* The Chinese University of Hong Kong, School of Architecture
Rm. 201, Lee Shau Kee Architecture Building, School of Architecture,
The Chinese University of Hong Kong, Shatin, Hong Kong
shuaizhongwang@cuhk.edu.hk

Abstract

Traditional gabions are limited by geometric rigidity, susceptibility to deformation, and underutilisation of granular pressure as a generative design parameter. This research introduces the bending-active gabion, a novel hybrid structural system that transforms passive containment into a form-active, self-equilibrated module for upcycling demolished concrete rubble. By integrating bending-active rods, tension cables, and concrete rubble infill, outward granular pressure is used as an active agent in the form-finding process rather than a passive load to be resisted. The methodology is structured as a three-phase digital-to-physical workflow. First, a computational form-finding framework based on Combinatorial Equilibrium Modelling (CEM) is developed to simulate equilibrium states, followed by multi-objective optimisation to minimise residual moments and maximise fill utilisation. Next, a 1:1 physical prototype was constructed using Glass-Fibre Reinforced Polymer (GFRP) rods arranged in a hexagonal prism configuration and filled with concrete rubble. Finally, the prototype was digitised via LiDAR scanning for quantitative evaluation. The validated results demonstrate that bending-active gabions offer a material-efficient, architecturally expressive pathway for circular construction, effectively transforming waste concrete into structurally performative components.

Keywords: bending-active, gabions, computational form-finding, concrete upcycling, circular construction

1. Introduction

Gabion systems are containers filled with granular materials used to protect banks or build retaining walls. Having long been valued for their cost efficiency, permeability, and durability, gabion systems are widely applied in retaining walls, hydraulic structures, dams, and marinas, with gabion cages shaped as regular boxes, flat mattresses, and tubular sacks (Figure 1) [1], [2], [3]. Notable examples of architectural projects include Herzog and de Meuron's Dominus Winery, BCHO Architects' Hanil Visitors Centre [4], [5], showcasing its unique design value and aesthetics. From a circularity standpoint, Gabion systems also serve as an effective pathway to upcycle demolished concrete rubble into structurally stronger construction components. While upcycling is preferred over downcycling and equivalent reuse in enhancing the structural capacity of resources [6], gabion system provides an even more cost-effective and convenient construction method compared to other concrete upcycling methods like dry stacking and grouted stacking [7], [8]. Although studies on using concrete rubble in gabion cages remain limited, relevant research into replacing conventional rocks with construction waste and coal bottom ash for gabion infill has shown promising results, demonstrating that gabions are an effective method of reusing waste [9], [10]. This research progress adds to the value of further research into more efficient gabion systems.

Copyright © 2026 by < Kwong Lau HUNG and Shuaizhong WANG >
Published by the International Association for Shell and Spatial Structures (IASS) with permission.



Figure 1: Common applications include gabion walls, gabion mattresses, and gabion sacks [11], [12], [13]

Despite their widespread use and benefits, the containment logic behind traditional gabion systems remains fundamentally passive. It exhibits three major shortcomings that limit the evolution of gabions towards more efficient and adaptable structural systems. Firstly, traditional gabions typically rely on fixed, box-shaped geometries. This disconnection between form and force flow leads to structural inefficiency. Research shows that gabion cages in hexagonal prism form, for instance, offer superior structural integrity against deformation and collapse [14]. This indicates that form-force optimisation is possible but remains underexplored in current gabion designs. Secondly, the passive containment of the gabion walls is prone to deformation. Gabion walls do not actively resist the outward pressure of the infill. Common failure modes include mesh breakage and infill breakage [15], revealing that the granular material is treated solely as a dead load rather than as a source of potential energy that could be balanced with other actively formed elements. Thirdly, the granular pressure of the gabion infill is treated solely as a dead load rather than an active design parameter. This misses the opportunity to control the granular pressure that could be harnessed to shape the container. The gabion system without this mechanism remains fundamentally limited in formal design freedom, requiring heavier cages and more material to resist forces that could otherwise be balanced.

Addressing the above gaps requires a fundamental shift from a passive containment logic to a form-active approach of gabion design. Bending-active structures that utilise the elastic deformations of originally straight elements to achieve curved geometries [16], offer unique advantages that directly respond to limitations of conventional gabions. With the ability to achieve high formal freedom with relatively minimal material, bending-active structures can overcome the geometric rigidity of traditional box-shaped gabion cages, enabling more complex, load-responsive geometries that align with internal force flow, directly addressing the inefficiency of fixed box-shaped gabions. Furthermore, the residual stress stored in elastic rods actively resists the outward pressure of the granular fill. Rather than relying solely on the tensile capacity of a mesh container, which is prone to bulging and failure, the system creates a self-equilibrated system where internal bending stress and tension cables balance outward pressure to maintain structural stability. Moreover, this approach allows the final shaping of the module to be determined by the outward pressure of the granular fill, turning the role of the infill from a mere dead load to a generative design driver that actively participates in form-finding. This synergy between material elasticity and granular mechanics ultimately transforms the gabion into a self-stabilising system, offering a high-performance framework for the efficient upcycling of demolished concrete rubble into material-efficient and formally expressive components.

2. Research Objectives

This research aims to develop and validate a new conceptual design methodology for a bending-active gabion hybrid that fundamentally redefines the structural role of the gabion from a passive container to a form-active, self-equilibrated system. The core contribution lies in proposing a new validated method for circular construction by demonstrating that the strategic integration between bending-active GFRP rods, tension cables, and upcycled concrete waste can generate performative, material-efficient, and

architecturally expressive structures, addressing the structural inefficiencies and limited design freedom of conventional gabion systems.

3. Methodology

The research follows a three-phase methodology: computational form-finding, physical prototyping, and quantitative evaluation (Figure 2). The workflow is designed to iteratively align digital simulation with physical reality, enabling the development and validation of a novel bending-active gabion hybrid.

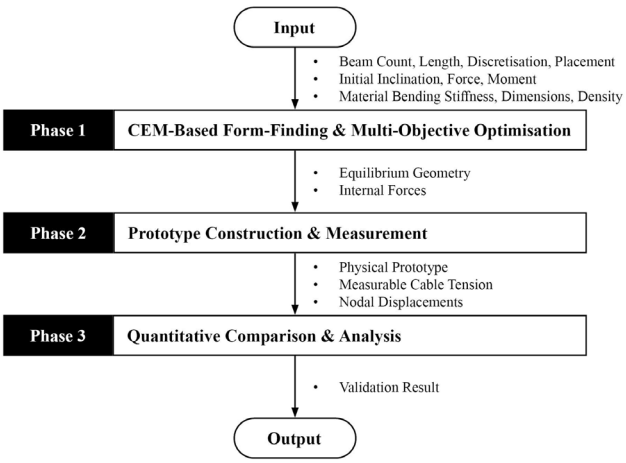


Figure 2: A digital-to-physical validation framework

3.1. Phase 1: Computational Form-Finding & Optimisation

Phase 1 develops a computational form-finding framework to simulate the equilibrium state of the bending-active gabion system. Utilising Combinatorial Equilibrium Modelling (CEM), the workflow equilibrates the residual bending stress from GFRP rods and cable tension against the granular pressure of concrete rubble. Multi-objective optimisation then refines the geometry to minimise residual moments and maximise the functional volume of the upcycled fill.

3.1.1. Form-Finding for Bending-Active Beams Using Graphic Statics and CEM

The form-finding of the bending-active gabion system is established through a framework that synthesises Graphic Statics and CEM. Following the methodology by Boulic, the system integrates bending behaviour by introducing a pair of equal and opposite forces acting on the nodes of the structural trail to represent internal bending moments [17]. This approach allows the conventional axial logic of graphic statics to simulate the elastic deformation and internal stresses of flexible members by incorporating material properties such as the Young's Modulus (E) and Second Moment of Inertia (I). Moreover, it leverages the transparency of graphic statics to provide a direct geometric relationship between form and internal forces, facilitating the intuitive manipulation of structural equilibrium without complex numerical iterations.

This principle is further integrated into the form-finding logic of CEM, which begins with the initialisation of a topological diagram (T). This diagram consists of trail edges and deviation edges organised in a hierarchical network. This system then undergoes a sequential derivation process of force equilibrium from origin vertices to support vertices along the sequence (k). This process calculates the location of the structural nodes and the internal forces of the system in equilibrium [18]. This integration offers detailed control of topology, loads, boundary conditions, and metric parameters from the user, which makes the form-finding of valid structural equilibrium states for a bending-active gabion fast, interactive, and intuitive for early conceptual design explorations.

3.1.2. Input Variables and Setup of Structural Simulation

Input variables include the material, geometry, and force description of the initial simulation setup. Material properties such as Young's Modulus (E) and Second Moment of Inertia (I) contribute to the bending stiffness of the elastic beam according to Euler-Bernoulli beam theory, and rubble bulk density (ρ) determines the degree of pressure exerted on the gabion walls. Geometrical input, such as the number of trails, position of origin points, and initial directions, determines the initiation of trail members, whereas the force input initiates the first force reciprocal.

Based on these inputs, the initial state of the computational model is configured as a simple tubular form (Figure 3) detailed as follows:

1. GFRP rods of 4 mm in diameter, 520 mm in length, are placed on the 6 vertices of a regular hexagon with a circumradius of 225 mm. The initial orientation (θ) of all rods is 60 degrees from the ground with zero moment applied onto the starting end.
2. Each rod is subdivided into 8 segments at 65 mm intervals. At each segment level, vertices are connected to adjacent rods via cable constraints, forming a horizontal ring. This discretisation allows for the application of distributed granular pressure as concentrated nodal forces.
3. Concrete rubble is modelled as a homogeneous granular material with a bulk density (ρ) of 1200 kg/m^3, representing upcycled aggregate from demolition waste.

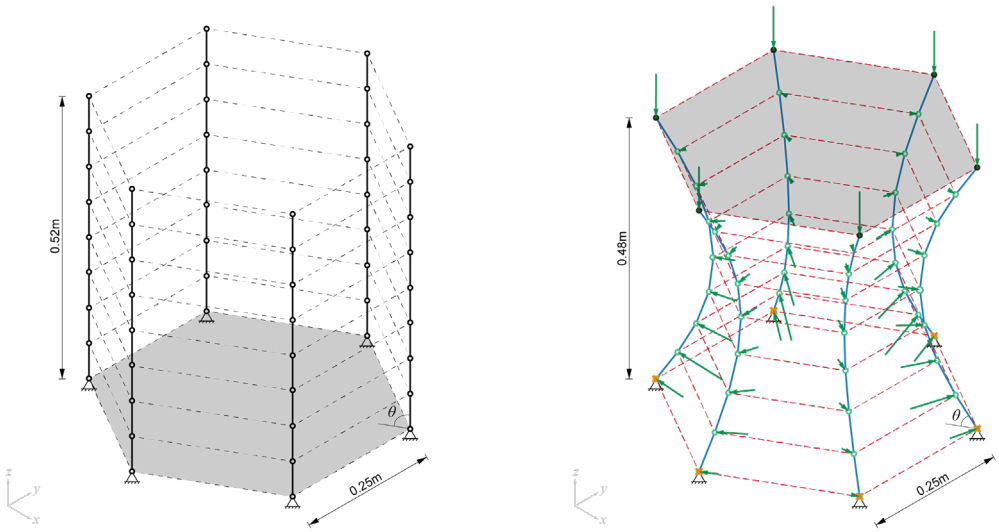


Figure 3: a) Structural simulation setup; b) Form-finding result based on principles of CEM

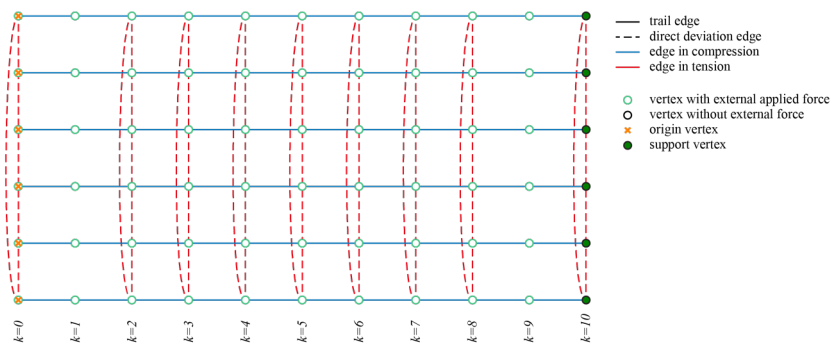


Figure 4: Topological diagram (T) of the simulated gabion system

3.1.3. Rubble Load Application Principle

To simulate the outward pressure exerted by the infill on the gabion wall, the research has opted for a linear hydrostatic pressure model in (1) as a simplified baseline for this preliminary study before introducing the complexity of internal friction. This equation is used to determine the magnitude of outward unit pressure (p) in Pascals for the infill at a given depth beneath the fill surface (h) in m, where the bulk density of the infill (ρ) is 1200 kg/m^3 and gravitational acceleration (g) is 9.81 m/s^2.

$$p = \rho g h \tag{1}$$

To distribute the outward pressure from the container surface to the nodes, each facet of the container is subdivided into four quadrilateral patches corresponding to its segment length (Figure 5a). For computational efficiency, the pressure is assumed to be constant and calculated at mid-height across each segment. This stepwise approximation is expected to converge with increased segment resolution.

$$\boldsymbol{P} = p \cdot A \tag{2}$$

The pressure force ($\boldsymbol{P}$) acting on each tributary surface equals its unit pressure (p) times surface area (A) as notated in (2), pointing outward along the surface normal. The total pressure force ($\boldsymbol{F_p}$) at each vertex is therefore the vector sum of pressure forces from its adjacent tributary surfaces in (3) (Figure 5b).

$$\boldsymbol{F_p} = \boldsymbol{P_1} + \boldsymbol{P_2} + \boldsymbol{P_3} + \boldsymbol{P_4} \tag{3}$$

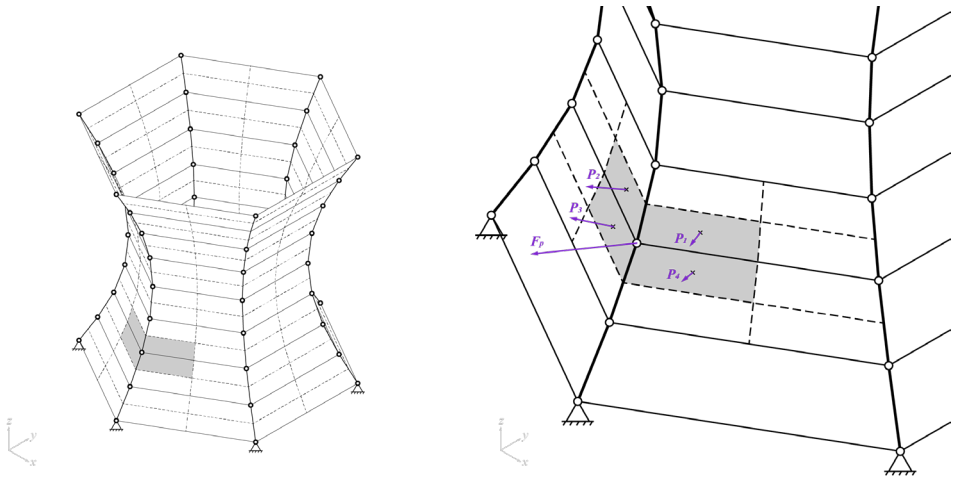


Figure 5: a) Schematic of assigning tributary surfaces; b) Calculation of nodal force induced by rubble pressure

3.1.4. Multi-Objective Optimisation

To explore more formal variations and identify optimal structural configurations, Wallacei, a multi-objective optimisation solver for Grasshopper based on Evolutionary Algorithms (EA), is deployed [19]. Optimisation variables include supporting forces at the base of each bending-active beam, internal force of tension cables, and the depth of the granular infill.

There are two objectives for the optimisation process: 1) Minimise the residual bending moment at the end of the bending-active beam to describe a pinned connection; 2) Minimise the level difference between the depth of the rubble fill and the height of the gabion to ensure full utilisation of the bending-active elements across its length. This optimisation process generates a Pareto front of non-dominated solutions, from which a balanced configuration is selected for physical prototyping. It was found that the time required for optimisation and its results are highly sensitive to the initial user input and the variable's domain, which should be improved in future studies.

3.2. Phase 2: Physical Prototyping of Bending-Active Gabion

In Phase 2, a 1:1 physical prototype is constructed to test and validate the computational form-finding model. The prototype replicates the geometry, material properties, and sequential formation process derived from the computational simulation.

3.2.1. Mechanical Properties of Prototype Materials

To materialise the results of the digital simulation, Glass-Fibre Reinforced Polymer (GFRP) is chosen as the material for the elastic rods due to its high strength-to-weight ratio, elastic deformability (low stiffness with high yield strength), and corrosion resistance. The GFRP rods used are 4mm in diameter with solid circular sections and a specified Young's Modulus of approximately 50 GPa. The upcycled concrete rubble sourced from a construction site on campus, with diameters ranging from 50 to 200 mm, is used as the granular agent for the prototype. A 10 L container (0.01 m^3) filled with rubble is weighed using a weighing scale to calibrate the bulk density as 1200 kg/m^3 (Figure 6). Galvanised steel wires with 1mm diameter are used for tension cables, providing adjustable tensile constraints for the framework. Generic construction meshes are used for the containment fabric to prevent smaller rubble pieces from escaping the gabion volume. The aforementioned material properties are then used to update the input variables in the form-finding algorithm accordingly.



Figure 6: a) Concrete rubble collected from the construction site on the campus; b) Rubble dimensions ranging from 50-200mm; c) Bulk density of rubble calculated by weighing sample rubbles in a 10L bucket

3.2.2. Connection Hardware

Several types of off-the-shelf hardware are used for the connection between components (Figure 7). For the support, stainless-steel ball-and-socket joints are used to connect the GFRP beams to the plywood model base, enabling free rotation and tilting within the fixed position. Stainless-steel cross-joints with tightening screws are used to allow for an adjustable connection between the GFRP beams and steel cables. Tension cables tied between the same level of vertices are designed to be continuous, with the two ends connected using a tightening connector to close the loop.



Figure 7: Three types of off-the-shelf connection hardware, including a) Stainless-steel ball-and-socket joint; b) Stainless-steel cross-joint; c) Steel cables and tightening connector

3.2.3. Construction Sequence of Physical Prototype

The final structural equilibrium is designed to be achieved through procedurally loading the system during the construction sequence. The sequence is described as follows (Figure 8):

1. The assembly begins with six elastic beams arranged in a regular hexagon. These beams are anchored to the model base using stainless-steel ball-and-socket joints, providing the necessary degree of freedom for deformation. Steel cables are then threaded and locked at fixed lengths between adjacent vertices in their corresponding levels. By tensioning the final set of cables tied to the boundaries of each beam, the beams are drawn into a prestressed bow shape, storing the elastic energy required to counteract the subsequent granular pressure applied.
2. The containment mesh is fabricated by sewing flat fabric according to the unrolled geometric pattern derived from the gabion geometry. This mesh is inserted into the framework and secured to the GFRP rods using zip ties. This layer acts as the skin to transfer the outward pressure of the concrete rubble to the bending active frame and prevent small rubble from falling out.
3. The final equilibrated geometry is achieved through the simultaneous placement of upcycled concrete rubble and real-time adjustment of the framework position. As the rubble is tightly packed, its internal pressure engages the tension cables and the elastic resistance of the bending-active rods. This process transforms the rubble from a passive dead load into a functional structural agent, resulting in a self-equilibrated state where residual bending stresses balance the granular outward pressure.

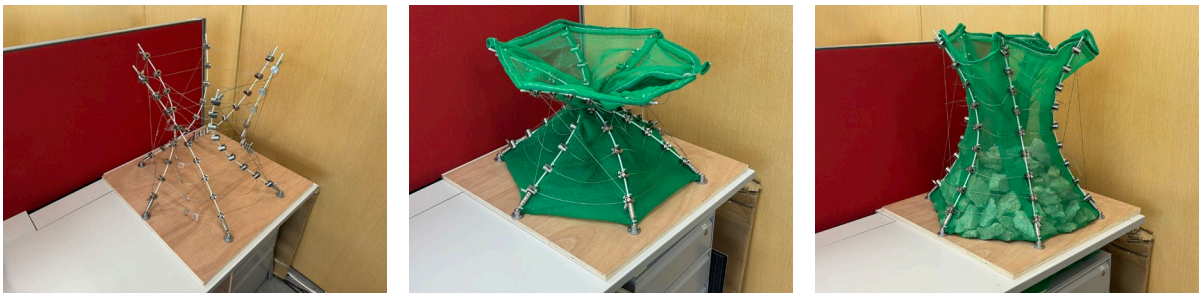


Figure 8: a) Step 1: Prestressing of bending-active beams; b) Step 2: Mesh inlay and surface attachment; c) Step 3: Concrete filling and equilibrium stabilisation

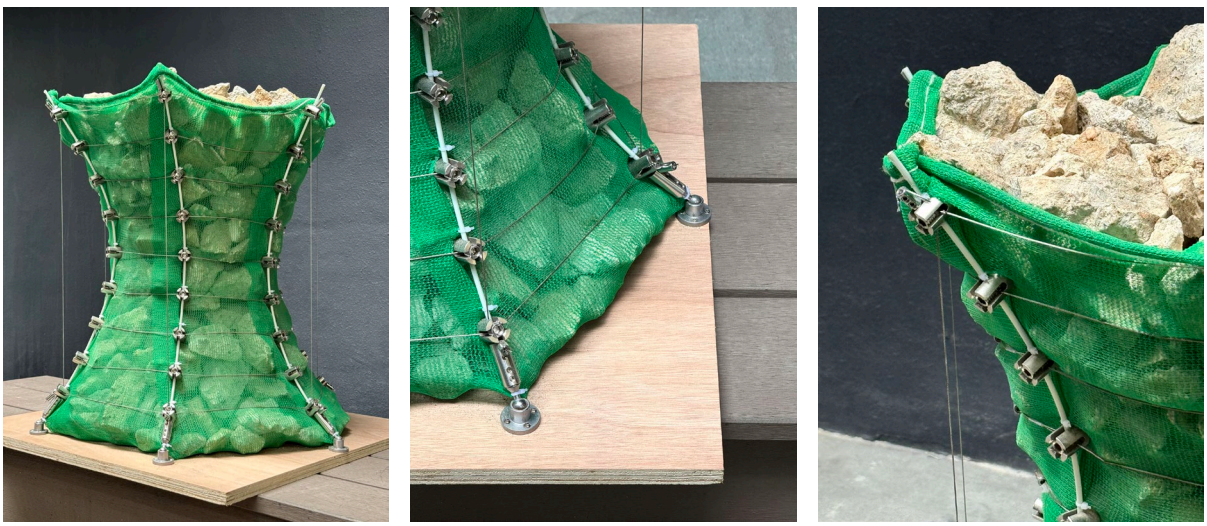


Figure 9: Photos of the 1:1 physically constructed prototype

3.3. Phase 3: Quantitative Evaluation

To validate the geometrical accuracy of the computational model against the constructed prototype and bridge the gap between digital simulation and physical reality, the physical prototype is digitised into a high-resolution mesh model using Polycam, a LiDAR-based 3D-scanning software for handheld iOS devices. The digitised mesh was then imported into the Rhino Grasshopper environment for processing and analysis. The process involves several key technical steps, including the alignment of the scanned mesh to the digital model using the base plate as reference, followed by the extraction of centrelines from the 3D-scanned GFRP rods to enable direct comparison with the simulated geometry. The following section evaluates three key aspects of geometrical discrepancies:

1. Nodal displacement was measured as the distance between the simulated vertices and the corresponding coordinates on the scanned prototype (nine nodes per elastic beam). As shown in the box plot (Figure 11a), nodal displacement varies across the full length of the beam, ranging from approximately 1 mm to 24 mm, which translates to about 4.8% of the total beam length. The variance could primarily be attributed to the manual assembly and filling process.
2. The deviations in bending curvature were evaluated by comparing the bending radius (R) of the extracted centreline in the physical model against the simulated geometry. Both digital and physical samples approximately follow the trend, with R highest at the boundaries of the beam and tightest in the central segment. The range of deviation falls approximately at ± 0.2 m from the simulated geometry, with the tightest R being ~ 0.2 m at Node 4 of Beam 2, within the bending capacity of the material before yielding (Figure 11b).
3. The volumetric accuracy was assessed by comparing the scanned volume filled with concrete rubble against the simulated volume of the gabion. The physical prototype exhibits a 7.8% volumetric deviation, equivalent to approximately 0.005 m^3 of extra volume.

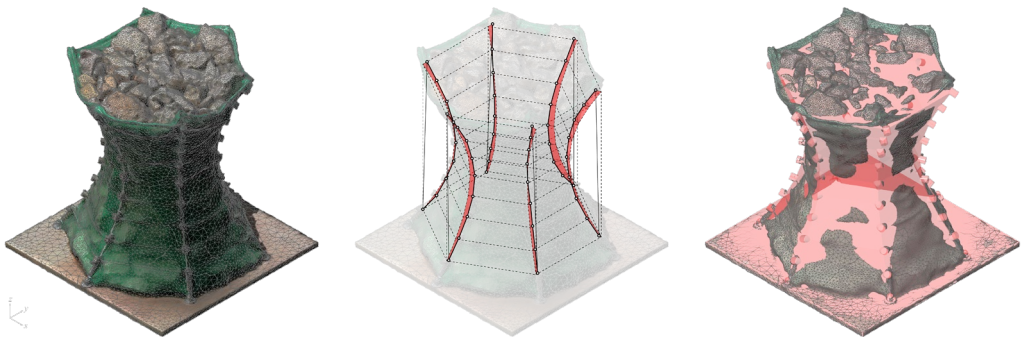


Figure 10: a) 3D-scanned mesh model generated by Polycam; b) Nodal displacement of physical prototype against simulated geometry; c) Volumetric overlay between simulated geometry and physical prototype

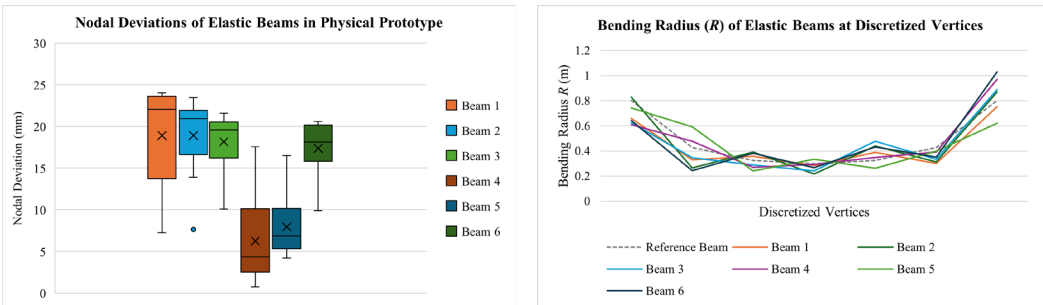


Figure 11: Box plots showing the distribution of (a) Nodal displacement and (b) Deviation of bending radius (R), measured at the discretised vertices on the bending-active beams

4. Discussion

The experimental results validate the transition of gabion systems from passive containers into form-active hybrids with meaningful discrepancies between the simulated geometry and the fabricated prototype. These measured discrepancies could be analysed and improved in the following ways:

1. Modelling Assumptions: The calculation of outward pressure exerted by the rubble onto the wall of the prototype was preliminarily assumed to follow linear hydrostatic pressure. However, with internal friction and particle interlocking between rubble pieces, it is more likely to follow granular pressure formulas such as Janssen's theory, which display nonlinear pressure across the container height. The irregular size and distribution of upcycled concrete rubble (50-200 mm) with non-uniform internal voids and unpredictable contact points likely caused an eccentric distribution of outward pressure, resulting in the uneven distribution of nodal displacement (reflecting a slight tilt of the central axis) observed in the physical prototype.
2. Fabrication Constraints: Several material and assembly constraints could potentially contribute to the discrepancies. The flexible containment mesh has shown a "bulging" effect and localised stretching between the elastic beams that alters the intended volumetric boundary, which could be mitigated by increasing the number of GFRP rods along the perimeter. The stainless-steel cross-joints introduced local rigidity, preventing the GFRP beams from achieving the predicted curvature. Other factors, such as assembly inaccuracies during manual bending of GFRP rods and hand-tensioning of cables, also led to the cumulative geometric drift.
3. Measurement Error: Handheld 3D scanning via the LiDAR-based Polycam App has an inherent margin of error, which could create slight geometric inaccuracies. The manual extraction of the centreline in the current method might also introduce further discrepancies, which could be improved in future processes by using positional sensors attached to the structural nodes evaluated with Iterative Closest Point (ICP) algorithms for more precise and reliable geometry matching.

These identified discrepancies and improvements underscore the complexity of combining non-standard upcycled materials with precise bending-active frameworks. Rather than undermining the structural validity of this system, it highlights the importance of developing a more robust digital-to-physical feedback loop that anticipates and integrates inherent material irregularity and construction constraints.

5. Conclusions

Overall, this research developed and validated a design methodology for bending-active gabion hybrids. Using a CEM-based computational form-finding model and 1:1 physical prototyping, it validated a digital-to-physical framework that utilises the granular pressure of upcycled concrete rubble as an active generative agent for stabilising the structural form, and bending-active GFRP beams to resist the pressure through residual stress, reducing the need for heavy rigid cages. The LiDAR-based evaluation also provides a viable method for establishing a feedback loop that iteratively refines the digital model to account for the inherent irregularities of reclaimed materials.

Future research will focus on overcoming the limitations of form-finding and fabrication in the current model to extend the design freedom into more complex structural forms. The preliminary linear pressure assumptions will be replaced with more advanced granular formulas, such as Janssen's theory, to more accurately calculate granular pressure under internal friction and particle interlocking. Further studies will explore a wider range of rotationally asymmetrical units and the integration of compression members to enable more complex free-form structural topologies. The implementation of VR-assisted construction will ensure real-time alignment between the simulated geometry and the constructed form in larger-scale applications, with sequential overlays guiding the construction sequence and reducing displacement errors in the current model. The feasibility of aggregating individual bending-active modules into larger load-bearing structures, such as free-standing retaining walls or vaulted structures, will also be explored to further enrich its formal variety.

References

[1] G.-L. Yang, Z.-Z. Liu, G.-L. Xu, and X.-J. Huang, 'Protection Technology and Applications of Gabion', in *Advances in Environmental Geotechnics*, Y. Chen, L. Zhan, and X. Tang, Eds, Berlin, Heidelberg: Springer Berlin Heidelberg, 2010, pp. 915–919. doi: 10.1007/978-3-642-04460-1_120.

[2] S. Y. Shah, Z. U. Islam, and S. A. Rather, 'Engineering feasibility of gabion structures over reinforced concrete structures', *Int. Res. J. Eng. Technol. IRJET*, vol. 05, no. 10, 2018.

[3] B. Toprak, O. Sevim, and I. Kalkan, 'GABION WALLS AND THEIR USE', *Int. J. Adv. Mech. Civ. Eng.*, vol. 3, no. 4, 2016.

[4] '137 Dominus Winery', Herzog & de Meuron. Accessed: May 07, 2026. [Online]. Available: https://www.herzogdemeuron.com/projects/137-dominus-winery/

[5] 'Hanil Visitors Center & Guest House / BCHO Architects', ArchDaily. Accessed: May 07, 2026. [Online]. Available: https://www.archdaily.com/72484/hanil-visitors-center-guest-house-bcho-architects

[6] C. Küpfer, M. Bastien-Masse, and C. Fivet, 'Reuse of concrete components in new construction projects: Critical review of 77 circular precedents', *J. Clean. Prod.*, vol. 383, p. 135235, Jan. 2023, doi: 10.1016/j.jclepro.2022.135235.

[7] R. L. Johns *et al.*, 'Autonomous dry stone', *Constr. Robot.*, vol. 4, no. 3, pp. 127–140, Dec. 2020, doi: 10.1007/s41693-020-00037-6.

[8] B. Wibranek and O. Tessmann, 'Digital Rubble Compression-Only Structures with Irregular Rock and 3D Printed Connectors', 2019.

[9] M. W. Kang, D. H. Moon, H.-S. Roh, Y. Jeon, H. Fu, and S. S. Lee, 'Innovative upcycling gabions with coal bottom ash for nonpoint source pollution control against climate change', *J. Clean. Prod.*, vol. 478, p. 143955, Nov. 2024, doi: 10.1016/j.jclepro.2024.143955.

[10] J. A. Paschoalin Filho, D. G. Camelo, D. De Carvalho, A. J. Guerner Dias, and B. A. Marcondes Versolatto, 'Use of construction and demolition solid wastes for basket gabion filling', *Waste Manag. Res. J. Sustain. Circ. Econ.*, vol. 38, no. 12, pp. 1321–1330, Dec. 2020, doi: 10.1177/0734242X20922591.

[11] Concertina Razor Wires LLC., 'Sack Gabion: Flexible Solution for Emergency and Erosion Control'. Accessed: May 05, 2026. [Online]. Available: https://www.concertinarazorwires.com/u/sack-gabion-52.html

[12] Gabionet Environment Solution, 'Gabion Mattresses'. Accessed: May 05, 2026. [Online]. Available: https://gabionet.com/gabion-mattresses/

[13] Terrock, 'From walls to planters: innovative gabion basket projects'. Accessed: May 05, 2026. [Online]. Available: https://terrock.co.uk/from-walls-to-planters-innovative-gabion-basket-projects/

[14] M. Ramli, T. J. r. Karasu, and E. T. Dawood, 'The stability of gabion walls for earth retaining structures', *Alex. Eng. J.*, vol. 52, no. 4, pp. 705–710, Dec. 2013, doi: 10.1016/j.aej.2013.07.005.

[15] H. Zhang, G. Liu, W. Liu, Z. Chen, Q. Liu, and G. Xu, 'Experimental study on failure mode and mechanical characteristics of gabion material', *Constr. Build. Mater.*, vol. 344, p. 128119, Aug. 2022, doi: 10.1016/j.conbuildmat.2022.128119.

[16] J. Lienhard, 'Bending-active structures: form-finding strategies using elastic deformation in static and kinetic systems and the structural potentials therein', PhD Thesis, ITKE, Stuttgart, 2014.

[17] L. Boulic, 'Form-Driven Design of Bending-Active Tensile Structures in Architecture', PhD Thesis, ETH Zurich, Zurich, Switzerland, 2019. doi: 10.3929/ETHZ-B-000421084.

[18] P. O. Ohlbrock and P. D'Acunto, 'A Computer-Aided Approach to Equilibrium Design Based on Graphic Statics and Combinatorial Variations', *Comput.-Aided Des.*, vol. 121, p. 102802, Apr. 2020, doi: 10.1016/j.cad.2019.102802.

[19] M. Makki, M. Showkatbakhsh, and S. Yutao, 'Wallacei: an evolutionary and analytic engine for grasshopper 3D'. Accessed: May 07, 2026. [Online]. Available: https://www.wallacei.com